RETRIEVING THE LONGITUDINAL NONLINEAR TUNES FROM FCT MEASUREMENTS

J. Rausch*[1], A. Sherjan[1,2], G. Franchetti[1,2,3], B. Lorentz[2]
[1]Goethe University Frankfurt, Frankfurt, Germany
[2]GSI Helmholtz Centre for Heavy Ion Research, Darmstadt, Germany
[3]Helmholtz Forschungsakademie Hessen für FAIR, Frankfurt am Main, Germany

Abstract

In synchrotrons and storage rings, the longitudinal dynamics of bunched beams is crucial in understanding beam loss. A fast current transformer (FCT) can be used to monitor the longitudinal bunch distribution. We use consecutive FCT measurements to analyze the beam's oscillations in the RF bucket at the Experimental Storage Ring (ESR) at GSI. At varying amplitudes of oscillation, the tunes in the non-linear bucket are reconstructed and discussed.

INTRODUCTION

Motivation

During the Machine Development (MD) time 2025 at the ESR, an effort was made to evaluate and improve the optics model of the machine. Beam based optimization studies were undertaken to improve the optics [1] and determine the non-linear components of dispersion [2]. Investigations on the longitudinal dynamics were possible using FCT measurements that were taken during times when the optics of the machine [3] was untouched. The synchrotron tune can be extracted from this measurement data and compared to the expected values given by the optics model and the machine settings during measurements.

Synchrotron Tune

The synchrotron tune in a storage ring is given by the rotation frequency of the beam in the RF-bucket ν_s in relation to the revolution frequency ν_r

$$Q_s = \frac{\nu_s}{\nu_r} \, , \tag{1}$$

where Q_s is the tune for small oscillation amplitude, for larger phase it has amplitude dependent components. The equations of motion of one particle in the bucket, without acceleration and radiation losses are

$$\dot{\phi} = \frac{2\pi q}{\beta^2 T_r}\left(\alpha_p - \frac{1}{\gamma^2}\right)\frac{\Delta E}{E_0} \tag{2}$$

$$\Delta\dot{E} = -\frac{qV}{T_r}\sin(\phi) \tag{3}$$

with T_r the revolution time of the on-momentum reference particle.

For small values of phase ϕ, Eqs. (2) and (3) can be approximated linearly as the harmonic oscillator. For the storage case without acceleration this results in a synchrotron tune of

$$Q_{s,0} = \sqrt{\frac{qVh}{2\pi\beta^2 E}\left|\left(\alpha_p - \frac{1}{\gamma^2}\right)\right|} \, , \tag{4}$$

with V the cavity gap voltage, E the beam energy, h the harmonic number, α_p the momentum compaction factor, relativistic β, γ. For phases $\phi \neq 0$ where $Q_s \neq Q_{s,0} =$ const. the differential equations represent the model of a non-linear pendulum. Its period can be determined exactly by an infinite series [4]. For the non-linear tune this yields

$$Q_s = Q_{s,0}\left(\sum_{n=0}^{\infty}\left(\frac{(2n)!}{(2^n n!)^2}\right)^2 \sin\left(\hat{\phi}/2\right)^{2n}\right)^{-1} \, . \tag{5}$$

The presented measurements give an approximation of both the zero order synchrotron tune as well as the higher order components in the ESR and are compared to the theoretical model.

MEASUREMENT PROCEDURE

Beam and Machine Setup

The measurements have been made during the Machine Development time at the Experimental Storage Ring (ESR) at GSI. For the MD, $^{40}Ar^{18+}$ beam with an energy of 400 MeV/u was provided by SIS18. The beam was injected into the ESR, bunched and stored at the injection energy. Additionally the beam was cooled with the electron cooler, which could also be switched off during storage. The cavity was used for bunching with a very low RF amplitude of $V = 146.61$ V. The bunching frequency was chosen with harmonic number $h = 1$.

FCT

For retrieving the longitudinal distribution of the stored and bunched beam, the current signal of the beam was measured by a Fast-Current-Transformer (FCT). The longitudinal beam profile of a cooled vs. non-cooled beam is shown in Fig. 1a, where τ is the time window of continuous measurement.

In Fig. 1b many consecutive continuous measurements, as Fig. 1a, are performed automatically at equal times intervals, each identified by the starting time t. All consecutive measurements of Fig. 1b are referred to as one measurement set. With the bunch not centered in the bucket, the expected oscillation can be observed in Fig. 1b.

* rausch@iap.uni-frankfurt.de

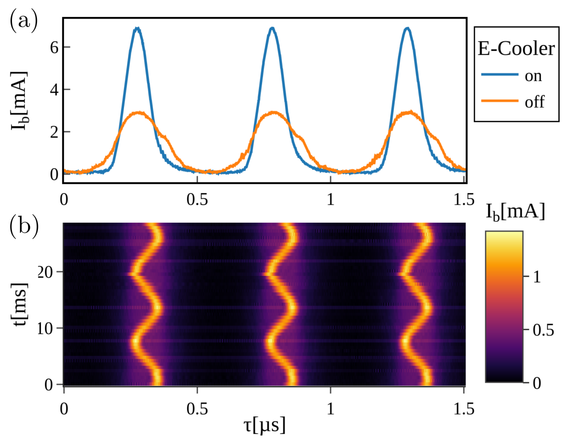

Figure 1: (a) Longitudinal beam profile measured with the FCT for cooled and uncooled beam at 400 MeV/u. The time window for each single profile measurement is chosen to include three turns. (b) Heatmap plot of one measurement set of the oscillating cooled beam.

METHODS

Fitting

The harmonic setting $h = 1$ and the time window τ, was chosen large enough to measure for more than one turn. The peaks of each single measurement (Fig. 1a) are found by a peak finding algorithm. We observe in Fig. 1a that the change of the longitudinal distribution of the beam in the time window τ ($\sim$ 3turns) is neglectable. Hence, the revolution frequency ν_r^{ex} is found by the distance of two consecutive peaks. This revolution frequency is also compared to the revolution frequency given by the set value of the cavity RF and the harmonic number. The oscillation of the peak of the beam profile is analyzed by fitting to the peak positions in Fig. 2 the sinusoidal function

$$\tau(t) = \hat{\tau} \sin\left[\omega_s (t + t_0)\right] + \tau_0 \ , \tag{6}$$

with the fitting parameters $\hat{\tau}$, τ_0, ω_s and t_0. Note that the offset t_0 accounts for the phase of the bunch in the bucket at the time when the first profile is measured while $\hat{\tau}$ is the amplitude of the oscillation of the beam center in the bucket.

Uncertainties in the Retrieved Quantities

For small oscillation amplitudes, the fit yields a high level of uncertainty for amplitude and frequency, because the amplitude of oscillation is near the random fluctuation of the trigger time of each profile measurement. The standard error $\sigma_i = \sqrt{\mathrm{Var}(p_i)}$ for each fit parameter p_i is calculated for each measurement set and is used as a criterion for which measurement sets to include for determining the synchrotron tune. The relative error of the fit parameter for the oscillation amplitude over the whole data set is shown in Fig. 3. Before analysis, data sets have been filtered by the threshold of uncertainties shown in Table 1 which set our selection criterion.

Table 1: Uncertainties σ Used as the Selection Criterion for the Fitting Data for Finding $\hat{\tau}$, ω_s, t_0 and τ_0

	$\hat{\tau}$	ω_s	t_0	τ_0
σ	< 0.03	< 0.03	< 0.01	< 0.01

Synchrotron Tunes

With the harmonic number h, the revolution frequency ν_r and the fit parameter for the bucket center τ_0, Eq. (6) can be transformed to an oscillation in cavity phase ϕ as follows

$$\phi = 2\pi h \nu_r (\tau - \tau_0) \ , \tag{7}$$

$$\phi(t) = \hat{\phi} \sin(\omega_s t + \varphi_0) \ . \tag{8}$$

Here ω_s is the angular frequency of the oscillation over the time t, φ_0 is the phase of the bunch oscillation at the first profile and $\hat{\phi}$ is the oscillation amplitude in cavity phase. An example of the detected peaks and the fitted oscillation is shown in Fig. 2. We repeated these sets of measurements to observe oscillations of varying amplitudes. The measurements were carried out both with cooled and non-cooled beam. The parameters retrieved from the fit of Fig. 2 for each measurement set, referred to by index m, are used to determine the oscillation frequency and therefore the synchrotron tune depending on the bunch oscillation amplitude. The measured synchrotron tune of the beam center Q_s^m is calculated from the synchrotron frequency ω_s^m retrieved from the fit by

$$Q_s^m = \frac{\omega_s^m}{2\pi \nu_r} \ . \tag{9}$$

Phase-Dependent Synchrotron Tune

From the fits for each measurement set the synchrotron tune is obtained from Eq. (9). All measurement sets give a collection of points $(\hat{\phi}, Q_s)_m$, which are used: 1) to fit an even polynomial series of the form

$$Q_s = Q_{s,0} + Q_{s,2}\hat{\phi}^2 + Q_{s,4}\hat{\phi}^4 + O\left(\hat{\phi}^6\right) \ , \tag{10}$$

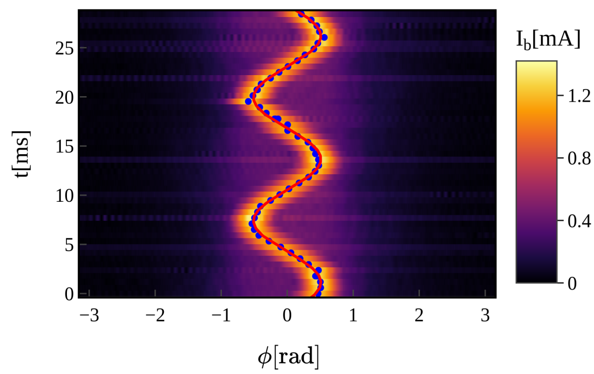

Figure 2: Heatmap of one measurement set, blue dots mark the peaks of each longitudinal profile. The red line is the fit of the sinusoidal along the peaks.

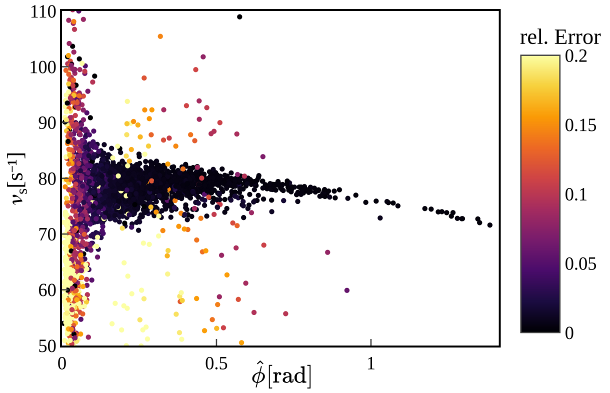

Figure 3: Plot of the fitted data points of the sets of measurements. The synchrotron frequency ν_s is plotted over the maximum cavity phase $\hat{\phi}$, i.e. the oscillation amplitude. The color of each dot represents the relative error of the amplitude fit parameter.

Table 2: Components of the Synchrotron Tune $Q_{s,n}$ According to Eq. (10) Fitted to the Measurement Data

n	0	2	4
$\mathbf{Q_{s,n}}$	4.074×10^{-5}	-2.13×10^{-6}	-1.4×10^{-7}
$\sigma_\mathbf{n}$	2.5×10^{-7}	6.3×10^{-7}	3.2×10^{-7}

from which we obtain the polynomial components and the amplitude dependency of the measured non-linear tune; 2) to fit the series representation of Q_s from Eq. (5). This series was calculated up to order 100 and is shown in Fig. 4. The two fit parameters are $Q_{s,0}$ and the harmonic number h used in the transformation of Eq. (7). With only integer values of the harmonic number h possible (and the machine set to $h = 1$), this fit parameter h can be used as a measure of accuracy of this fitting model.

RESULTS

Figure 4 shows the transformed data points of all measurement sets that fulfill the uncertainty selection criterion of Tab. 1. Since the spread of tune values is very large for small $\hat{\phi}$, the fitting was performed on all data points where $\hat{\phi} > 0.6$. In the picture is also shown (color cyan) the polynomial fit, Eq. (10) with the coefficients of Tab. 2. Figure 4 also shows (color magenta) the fit of the series representation, Eq. (5), which yields the following results

$$Q_{s,0} = 4.085(10) \times 10^{-5} \ , \ h = 1.025(26) \ . \qquad (11)$$

DISCUSSION

The phase-dependent synchrotron tune could be determined up to the fourth order. The uncertainty of the polynomial method however is large at $Q_{s,4}$. The harmonic number resulting from the fit of Eq. (5) matches the $h = 1$ integer, indicating that the non-linear model follows the measurement data closely.

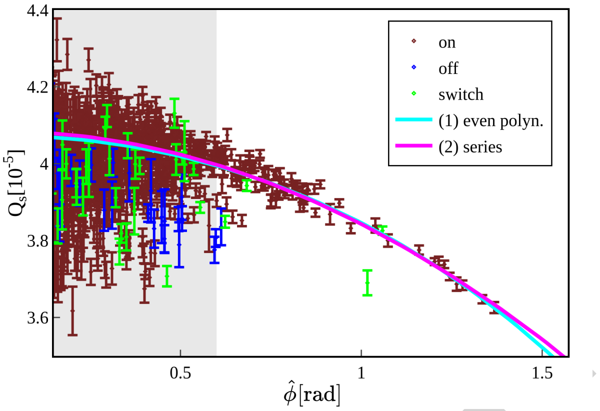

Figure 4: Plot of the synchrotron tune of all filtered data points and the two applied fit functions. The color of the points shows the status of the electron cooler during each measurement set. The error bars represent uncertainty of the frequency fit of each individual set. Only points in the white area are taken into account for the fitting.

The zero-order synchrotron tune $Q_{s,0}$ was determined with high confidence. The ESR model of the machine optics and the RF settings yield a momentum compaction of $\alpha_p = 0.1641$, and the calculated synchrotron tune of $Q_s^{\text{th}} = 1.293 \times 10^{-4}$, which significantly differs from the experimental findings in Table 2 and Eq. (11). In fact, the measurements averaging over both fit methods, give a resulting synchrotron tune of $\bar{Q}_{s,0} = 4.08 \times 10^{-5}$. We interpret this finding as follows: From Eq. (4) the dependence of Q_s on V, h, E, γ would be detectable through beam diagnostics, hence we infer that an inexact value of α_p might be the origin of the discrepancy.

Using the measured tune, and assuming that all other parameters are correct, the momentum compaction factor of the machine is estimated to be $\alpha_p = 0.457\,05$, which corresponds to a slip factor of $\eta = -0.032\,37$ contrarily to the theoretical value of $\eta = -0.3253$, suggesting the machine much closer to transition energy than expected.

CONCLUSION

We proposed a method to retrieve from bunch oscillations the phase dependent synchrotron tune. The analysis of the experimental data brought up discrepancies between the measured values and the expectations from the optics and machine settings. Future investigations into the longitudinal dynamics of the ESR including both simulations and dedicated measurements are necessary to understand the underlying effects.

ACKNOWLEDGEMENTS

We thank O. Chorniy for the support on beam diagnostics tools and the ESR group for preparing the machine.

REFERENCES

[1] A. Heinz *et al.*, “Beam-based optimization of the ESR linear optics model”, presented at IPAC’26, Deauville, France, May

2026, paper WEP5015, this conference.

[2] A. Sherjan, G. Franchetti, and J. Rausch, “Measurements and studies on the nonlinear Dispersion in the ESR”, presented at IPAC’26, Deauville, France, May 2026, paper THP4076, this conference.

[3] B. Franzke, “The heavy ion storage and cooler ring project ESR at GSI,”*Nucl. Instrum. Methods Phys. Res., Sect. B*, vol. 24-25, pp. 18–25, Apr. 1987. doi:10.1016/0168-583x(87)90583-0

[4] M. Abramowitz, I. A. Stegun, and D. Miller, “Handbook of Mathematical Functions With Formulas, Graphs and Mathematical Tables (National Bureau of Standards Applied Mathematics Series No. 55),”*ASME J. Appl. Mech.*, vol. 32, no. 1, pp. 239–239, Mar. 1965. doi:10.1115/1.3625776